Magnetic Scattering of Spin Polarized Carriers in (In, Mn)Sb Dilute Magnetic Semiconductor

M. Csontos,[1] T. Wojtowicz,[2,3] X. Liu,[2] M. Dobrowolska,[2] B. Jankó,[2] J. K. Furdyna,[2] and G. Mihály[1]

[1]*Department of Physics, Budapest University of Technology and Economics and "Electron Transport in Solids" Research Group of the Hungarian Academy of Sciences, 1111 Budapest, Hungary*

[2]*Department of Physics, University of Notre Dame, Notre Dame, Indiana 46556, USA*

[3]*Institute of Physics, Polish Academy of Sciences, 02-668 Warsaw, Poland*

(Received 24 May 2005; published 21 November 2005; corrected 14 December 2005)

Magnetoresistance measurements on the magnetic semiconductor (In, Mn)Sb suggest that magnetic scattering in this material is dominated by isolated Mn^{2+} ions located outside the ferromagnetically ordered regions when the system is below T_c. A model is proposed, based on the *p-d* exchange between spin-polarized charge carriers and localized Mn^{2+} ions, which accounts for the observed behavior both below and above the ferromagnetic phase transition. The suggested picture is further verified by high-pressure experiments, in which the degree of magnetic interaction can be varied in a controlled way.

DOI: 10.1103/PhysRevLett.95.227203 PACS numbers: 75.50.Pp, 72.25.Dc, 75.30.Et, 75.47.De

The presence of charge and spin degrees of freedom in III-Mn-V magnetic semiconductors alloys opens new perspectives for spintronic applications [1–3]. In these systems the Mn^{2+} ions provide $S = 5/2$ magnetic moments, and also act as a source of valence band holes that mediate Mn^{2+}-Mn^{2+} interactions. The interactions between the randomly positioned magnetic ions are predominantly ferromagnetic (FM), resulting in a low-temperature FM phase [4–9]. Thus the magnetic and the electrical transport properties of III-Mn-V materials are fundamentally interdependent. Although many aspects of free carrier magnetotransport have already been explored in these materials, its microscopic understanding is still far from complete. Recent scaling theory on Anderson-localized disordered ferromagnets applies to transport in the *localized* limit [10], but the more interesting ''metallic'' systems—where the mean free path satisfies the $k_F l \gg 1$ condition (where k_F is the Fermi wave number)—require a different approach.

Many spintronic applications envision spin injection and/or spin-polarized current, and are thus expected to hinge critically on our understanding of spin scattering of the charge carriers. In this Letter we present a detailed experimental study of magnetic scattering processes in the dilute magnetic semiconductor (In, Mn)Sb. We find that in the FM phase the positional disorder of the magnetic moments is reflected in the slowly saturating nature of both the magnetization and magnetoresistance. This suggests the presence of isolated Mn^{2+} ions located outside the FM-ordered regions. The large negative magnetoresistance observed below T_c is attributed to a first order magnetic scattering of spin-polarized holes on such isolated paramagnetic Mn^{2+} ions. Above T_c the spontaneous spin polarization of the carriers is lost and second-order spin-independent processes begin to dominate. This picture is supported by high-pressure measurements, in which the interaction between charge-carrying holes and localized Mn^{2+} ions can be experimentally varied [11].

In the present work we present results obtained on $In_{1-x}Mn_xSb$ for $x = 0.02$. Similar behavior has been found for other concentrations. More importantly, the same *qualitative* behavior has also been reported for the most widely studied magnetic semiconductor $Ga_{1-x}Mn_xAs$ [4,12]. We therefore believe that the results on (In, Mn)Sb reflect a common feature of highly conducting III-Mn-V magnetic semiconductors. While specific details of the spin landscape (FM-ordered regions and isolated Mn^{2+} spins) may vary from system to system, the great advantage of $In_{0.98}Mn_{0.02}Sb$ is that here the isolated Mn^{2+} ions can be unambiguously identified as the dominant source of the magnetic scattering.

The $In_{1-x}Mn_xSb$ films were grown by low-temperature molecular beam epitaxy (MBE) in a Riber 32 R&D MBE system on closely lattice-matched hybrid (001) CdTe/GaAs substrates to a thickness of about 230 nm [13]. [For further growth details and structural characterization, see Ref. [13]]. In the $In_{0.98}Mn_{0.02}Sb$ sample used in this study 80% of the Mn is magnetically active while the compensation by interstitial Mn is 5% [13]. These numbers are consistent both with the estimated saturation magnetization of about 13 emu/cm^3 (see Fig. 1) and with the hole concentration of $\approx 3 \times 10^{-20}$ cm^{-3} deduced from Hall effect measurements. At low temperatures the resistivity is typically 250 $\mu\Omega$ cm, corresponding to a metallic mean free path of $k_F l \approx 30$.

The magnetic properties were investigated by magnetic circular dichroism (MCD) and by superconducting quantum interference device (SQUID) measurements. The MCD signal was normalized to low-field SQUID data, with an accuracy of about 20%. Magnetotransport measurements were carried out in a six-probe arrangement, with magnetic field normal to the layer [14]. For high-pressure measurements the samples were mounted in a self-clamping cell, with kerosene as the pressure medium.

The field dependence of magnetization $M(B)$ obtained from MCD measurements is shown in the upper panel of

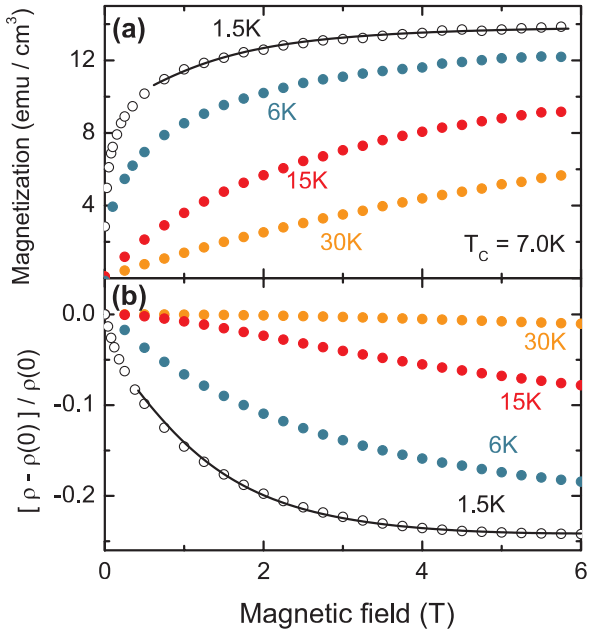

FIG. 1 (color online). Magnetization measured by magnetic circular dichroism (a) and reflected in magnetoresistance (b) as a function of the applied field up to 6 T. The Curie temperature is $T_c = 7$ K. The solid lines represent the $B_{5/2}$ Brillouin function characterizing the magnetization of isolated Mn^{2+} ions.

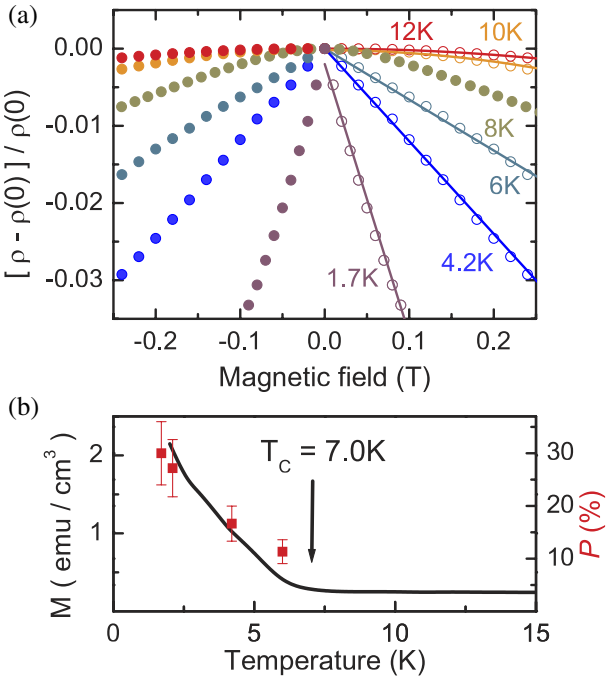

FIG. 2 (color online). (a) Low-field magnetoresistance, showing quadratic field dependence above T_c, and linear dependence in the FM phase. Solid lines are fits to the data according to the $B \to 0$ limits of Eqs. (3) and (4). (b) Remanent magnetization measured by SQUID as a function of temperature (solid line). The data points show the spin polarization of charge carriers deduced from the initial slope of the magnetoresistance below T_c (the absolute scale was determined by taking $J_{pd}/V = 0.17$, see text).

Fig. 1. At $T = 30$ K (well above the Curie temperature) $M(B)$ is seen to vary linearly with the applied field, as expected for a paramagnetic material. Below $T_c = 7$ K the almost steplike $M(B)$ curves resemble the magnetization of a FM material, but no saturation is reached up to a few Tesla. For example, at $T = 1.5$ K about 80% of the estimated saturation value is achieved at $B = 1$ T, and we relate this large value of M to the spin alignment within the FM-ordered regions of the system. On the other hand, the slowly saturating part superimposed on this FM magnetization clearly indicates that a fraction of the Mn^{2+} magnetic moments still remain isolated (i.e., are not included in the FM-ordered regions).

The magnetoresistance curves measured at the same temperatures and in the same field range are shown in the lower panel of Fig. 1. At high fields they exhibit a similar field dependencies as the corresponding magnetization curves. The simultaneous slow saturation observed in magnetization and in resistivity suggests that the magnetoresistance arises from a magnetic scattering process which is gradually "frozen out" as more isolated random Mn^{2+} spins become aligned. The analysis given below for the results in Figs. 2–4 shows that the field- induced alignment indeed follows a $B_{5/2}$ Brillouin function, clearly suggesting that the slow component of the saturation is closely related to the isolated Mn^{2+} spin population.

Figure 2 presents the magnetoresistance at low fields. Note that the quadratic behavior of ρ above the phase transition changes to linear as T is decreased below T_c. We shall show that the *linear* magnetoresistance observed in the FM phase indicates the presence of spin-polarized carriers in the scattering process. Specifically, such linear B dependence is *symmetry breaking*, and indicates that the polarization of the charge-carrying holes changes sign as B is reversed.

In the following we briefly discuss the expected behavior when spin-polarized carriers are scattered on isolated Mn^{2+} ions. The Hamiltonian for the interaction between delocalized holes of spin s and half-filled $3d$ shells of the Mn^{2+} ($S = 5/2$) ions is

$$H = V - 2J_{pd}\mathbf{s} \cdot \mathbf{S}, \tag{1}$$

where V is the spin-independent part of the potential, and the second term describes the exchange interaction described by the J_{pd} coupling constant [6,15]. The spin-dependent scattering on isolated (paramagnetic) Mn^{2+} ions can be described by a perturbation calculation in the limit $|J_{pd}| \ll V$. In the presence of a magnetic field the relaxation times $\tau_{\pm}$ for the spin-up and spin-down carriers is (up to second order in J_{pd}/V) given by [15]

$$\frac{1}{\tau_{\pm}} = C\left[1 \mp \frac{2J_{pd}}{V}\langle S_z\rangle + \left(\frac{2J_{pd}}{V}\right)^2 f(\langle S_z^2\rangle)\right], \tag{2}$$

where $\langle S_z\rangle$ is the average field-direction component given

by the $B_{5/2}(\alpha)$ Brillouin function with an argument of $\alpha = g\mu_B B/k_B T_{\text{eff}}$, $M = g\mu_B\langle S_z\rangle$ is the corresponding magnetization, while $f(\langle S_z^2\rangle)$ and C are given in Ref. [15].

In a system containing a few percent of Mn the p-d interaction defined in Eq. (1) couples the Mn^{2+} moments to each other via an RKKY-like superexchange [for details see Ref. [6]]. Since the carrier density is low, the first node of the oscillating RKKY function occurs at a length scale larger than the average Mn-Mn separation, giving rise to a net FM interaction, $J \propto J_{pd}^2$. Magnetic ordering in such spin landscape is somewhat unusual: according to Monte Carlo simulations [16] small FM-ordered regions in fact begin to develop *above* the mean-field T_c where the local Mn density exceeds the average. These regions increase as T decreases, eventually developing into a percolated network at T_c. However, a fraction of the spins can still remain outside this FM network even below T_c, and we suggest that these constitute the source of magnetic scattering.

In the FM phase the numbers of spin-up and spin-down carriers are different, so that the leading linear term in $\langle S_z\rangle$ does not cancel out in Eq. (2), and dominates over the second-order quadratic term. The difference between $1/\tau_+$ and $1/\tau_-$ then gives rise a nonvanishing $2\mathcal{P}\frac{2J_{pd}}{V}\langle S_z\rangle$ term, where $\mathcal{P}$ is the difference in the density of states of spin-up and spin-down subbands, i.e., the spin polarization of the charge carriers. Consequently, the first order magnetic scattering leads to a magnetoresistance that is proportional both to the spin polarization arising from the FM block and to the magnetization of the isolated paramagnetic moments:

$$\frac{\rho(B)-\rho(0)}{\rho(0)} = -4\mathcal{P}\frac{J_{pd}}{V}\langle S_z\rangle = -4\mathcal{P}\frac{J_{pd}}{g\mu_B V}M(B). \quad (3)$$

An important prediction of this Eq. (3) is that in the FM phase the magnetoresistance directly measures the magnetization of the isolated Mn^{2+} ions. This is verified by the high-field results shown in Fig. 3, where the continuous lines correspond to the $B_{5/2}$ Brillouin function describing the magnetization of isolated $S = 5/2$ spins. The argument of the Brillouin function is $\alpha = g\mu_B B/k_B T_{\text{eff}}$, where the effective temperature $T_{\text{eff}} = T + T_{\text{AF}}$ contains an empirical antiferromagnetic (AF) coupling parameter describing the natural AF interaction between Mn ions [6,17]. T_{AF} is the *only* fitting parameter used to describe the observed *magnetic field-temperature* scaling. The same (small) value $T_{\text{AF}} = 1.4$ K has been used to fit all curves.

At low T a quadratic contribution to the magnetoresistance gradually emerges. This is attributed to the ordinary positive magnetoresistance, and in the left panel of Fig. 3 it is subtracted at each temperature. The separation of the Brillouin and the quadratic terms is shown in the right panel of Fig. 3.

We believe that the $B_{5/2}$ Brillouin fits in Fig. 3 for the FM phase provide strong evidence for magnetic scattering of spin-polarized holes on isolated Mn^{2+} ($S = 5/2$) ions.

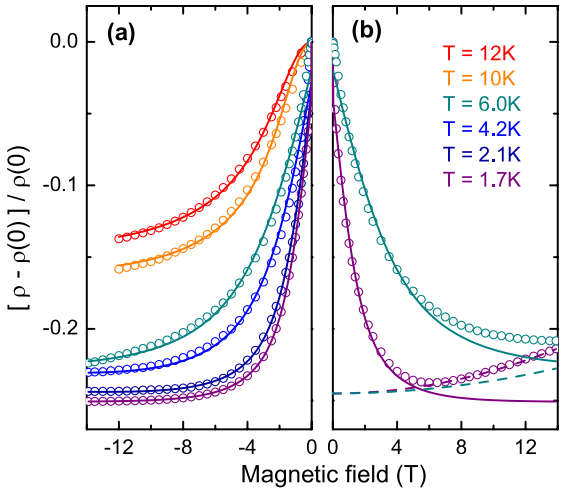

FIG. 3 (color online). Magnetoresistance measured up to 14 T at selected temperatures below (various blue curves) and above T_c (red and yellow curves). A positive quadratic term attributed to normal magnetoresistance is subtracted at each temperature, as shown in (b). Continuous lines in (a) correspond to Eqs. (3) and (4), with $\langle S_z\rangle$ given by the Brillouin function for $S = 5/2$.

Equation (3) also allows the estimation of the spin polarization from the low-field slope of the magnetoresistance curves, which is $\mathcal{P}(T)J_{pd}/Vg\mu_B B/k_B T_{\text{eff}}$. Comparison of the spin polarization obtained from transport experiments with remanent magnetization measured by SQUID is shown in the lower panel of Fig. 2. The $\mathcal{P}(T) \propto M_{\text{rem}}(T)$ relation in the FM phase provides additional support for the applied model.

Above T_c, i.e., in the paramagnetic phase, the global spin polarization is lost, and for $\alpha < 2$ (which is fulfilled for our experiments) the second-order term in Eq. (2) leads to magnetoresistance expressed by [15]:

$$\frac{\Delta\rho(B)}{\rho(0)} = -\frac{J_{pd}^2}{V^2}\left[4\langle S_z\rangle^2 + \langle S_z\rangle\left(\coth\frac{\alpha}{2} - \frac{\alpha}{2\sinh^2\frac{\alpha}{2}}\right)\right]. \quad (4)$$

Equation (4) accounts for the low-field quadratic variation of magnetoresistance above T_c seen in Fig. 2, as well as for its behavior over the broad magnetic field range shown in Fig. 3. Although a second-order term is expected to make a weaker contribution, the observed magnetoresistance is still very large, since in the paramagnetic phase most of the Mn ions take part in the scattering. In this picture we neglect fluctuations in the Mn concentration, and the ferromagnetic interaction between the Mn ions in the paramagnetic phase is expressed via an effective temperature T_{eff} for that phase, $T_{\text{eff}} = T - T^*$, where simple mean-field theory predicts T^* close to T_c. Note that T_{eff} is the only fitting parameter used in the calculations (the magnitude of the magnetoresistance gives the strength of the scattering: $J_{pd}/V \simeq 0.17$). The fits shown in Fig. 3 indeed yield T^* very close to $T_c = 7.0$ K: ($T^* = 6.2$ and $T^* = 7.1$ K for the orange and the red curves, respectively), thus providing support for the intuitive mean-field scenario.

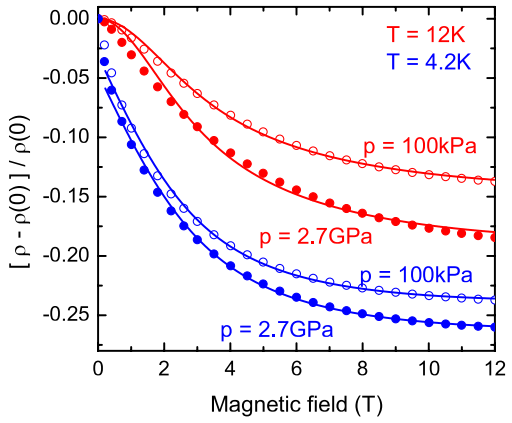

FIG. 4 (color online). Effect of hydrostatic pressure on magnetoresistance measured below (blue curve) and above T_c (red curve). Open symbols: ambient pressure; solid symbols: $p = 2.7$ GPa. Fits for ambient pressure are calculated using Eqs. (3) and (4); fits for pressure data are calculated using the same expression, with J_{pd} increased by 5.6%. In the paramagnetic phase we found that T^* is also enhanced by pressure (from 7.1 K to 7.6 K), as expected.

The validity of Eqs. (3) and (4) can be further tested by applying hydrostatic pressure to tune the exchange coupling J_{pd}. Earlier investigations on various magnetic semiconductors [6,18] indicated that the p-d exchange energy varies inversely as the volume v_0 of the unit cell, $J_{pd} \propto v_0^{-1}$. A clear pressure-induced enhancement of magnetoresistance is shown in Fig. 4 both below and above T_c. Using the bulk modulus of InSb ($\kappa = 48$ GPa) one expects a $\delta v_0/v_0 = p/\kappa = 5.6\%$ decrease in v_0 for the applied pressure of $p = 2.7$ GPa, and thus the same increase in J_{pd}.

In the FM phase magnetic scattering varies as the product of J_{pd} and $\mathcal{P}$, which itself varies as the strength of the J_{pd} coupling. Taking both effects into account, Eq. (3) predicts that below T_c magnetoresistance depends on the p-d coupling as J_{pd}^2. Accordingly, the application of $p = 2.7$ Gpa should result in an 11.2% enhancement of the magnetoresistance. Indeed, in Fig. 4 excellent agreement is obtained when we fit the high pressure $T = 4.2$ K data simply by applying this 11.2% magnification to the ambient fit (the fitting parameter T_{AF} is influenced only slightly: it increases by 0.38 K).

Above T_c one should—besides the J_{pd}^2 enhancement—also take into account the pressure-induced increase of FM coupling described by the parameter T^*. Fits of high-pressure data at 12 K indicate that T^* is indeed enhanced from 7.1 K to 7.6 K, providing additional support to the consistency of our picture.

In conclusion, the high-field and high-pressure transport experiments in (In, Mn)Sb revealed that the large magnetoresistance observed in this magnetic semiconductor is dominated by scattering on isolated Mn^{2+} ($S = 5/2$) ions. The qualitative changes (e.g., the change from quadratic to linear magnetoresistance as the temperature is lowered below T_c, or the freezing out of scattering as spins become aligned by an applied field) can all be described by the p-d interaction between charge-carrying holes and localized Mn moments. In the FM phase the magnetoresistance arises from scattering of spin-polarized carriers, its field dependence directly following the magnetization of the few ions that are not included in the FM order. Above T_c the spin polarization is lost and magnetic scattering becomes a second-order process, but now *most* Mn ions participate in the scattering, so that the magnitude of the effect remains large. Finally, by enhancing the strength of the p-d coupling by hydrostatic pressure, we also showed that the observed pressure-induced increase of magnetoresistance also follows directly from the above microscopic picture.

Valuable discussions with T. Dietl and G. Zaránd are acknowledged. This research has been supported by the Hungarian research funds OTKA TS049881 and the National Science Foundation NIRT Grant No. DMR 02-10519. B. J. was also supported by the Alfred P. Sloan Foundation.

[1] H. Ohno *et al.*, Nature (London) **408**, 944 (2000).
[2] D. Chiba, M. Yamanouchi, F. Matsukura, and H. Ohno, Science **301**, 943 (2003).
[3] M. Yamanouchi, D. Chiba, F. Matsukura, and H. Ohno, Nature (London) **428**, 539 (2004).
[4] H. Ohno, Science **281**, 951 (1998).
[5] T. Dietl *et al.*, Science **287**, 1019 (2000).
[6] T. Dietl, H. Ohno, and F. Matsukura, Phys. Rev. B **63**, 195205 (2001).
[7] J. König, J. Schliemann, T. Jungwirth, and A. H. MacDonald, in *Electronic Structure and Magnetism of Complex Materials*, edited by D. J. Singh and D. A. Papaconstantopoulos (Springer-Verlag, Berlin, 2002).
[8] T. Dietl, Semicond. Sci. Technol. **17**, 377 (2002).
[9] T. Jungwirth *et al.*, Phys. Rev. B **66**, 012402 (2002).
[10] G. Zaránd, C. P. Moca, and B. Jankó, Phys. Rev. Lett. **94**, 247202 (2005).
[11] M. Csontos *et al.*, Nat. Mater. **4**, 447 (2005).
[12] Y. Iye *et al.*, Mater. Sci. Eng. B **63**, 88 (1999).
[13] T. Wojtowicz *et al.*, Appl. Phys. Lett. **82**, 4310 (2003); T. Wojtowicz *et al.*, Physica (Amsterdam) **20E**, 325 (2004).
[14] Magnetic anisotropy observed in the ~0.01 T field range [see Ref. [13]] does not play a role in the high-field studies presented in this Letter.
[15] M.-T. Béal-Monod and R. A. Weiner, Phys. Rev. **170**, 552 (1968).
[16] R. N. Bhatt, M. Berciu, M. P. Kennett, and X. Wan, J. Supercond. **15**, 71 (2002).
[17] Y. Shapira *et al.*, Phys. Rev. B **33**, 356 (1986).
[18] T. M. Giebultowicz, J. J. Rhyne, J. K. Furdyna, and P. Klosowski, J. Appl. Phys. **67**, 5096 (1990).